Ore Geology Reviews 78 (2016) 138–150

Contents lists available at ScienceDirect

Ore Geology Reviews

journal homepage: www.elsevier.com/locate/oregeorev

Intrinsic geological model generation for chromite pods in the Sabzevar ophiolite complex, NE Iran

Mehrdad Soleimani [a], Behshad Jodeiri Shokri [b,*]

[a] Faculty of Mining, Petroleum and Geophysics, Shahrood University of Technology, Shahrood, Iran
[b] Department of Mining Engineering, Hamedan University of Technology, Hamedan, Iran

ARTICLE INFO

Article history:
Received 8 August 2015
Received in revised form 15 March 2016
Accepted 16 March 2016
Available online 6 April 2016

Keywords:
Chromite
Mathematical – geological genetic model
Intrinsic geological unit
Critical genetic factor
Critical reconnaissance criteria

ABSTRACT

The Sabzevar ophiolite, with its colored mélange zone, is a highly disintegrated ophiolite complex located at the northern boundary of the central Iranian microcontinent. A large number of chromite pods occur in this area, which needs to be explored. In this study, a mathematical – geological genetic model is advanced as an exploratory tool that provides information for further exploration activity. A petrogenetic model of chromite ore was established on the basis of a geodata information database. This database consists of information from similar chromite mines from around the world. A detailed investigation of the geological, mineralogical and petrological characteristics of chromite pods in the Sabzevar region was conducted along with detailed petrological samplings, thin section studies and mineralogical analysis. In the next step, we developed a conceptual genetic model that defines areas with a high probability of the existence of chromite pods. The model was later refined using such parameters as a critical genetic factor (CGF) and critical reconnaissance criteria (CRC). Next, a linear function, which is a combination of these factors, provided promising regions as intrinsic geological units (IGU). Finally, a 3D model of lithological units depicting the IGU for chromite pods exploration is proposed.

1. Introduction

On a regional scale, geological knowledge can be effectively represented and spatially queried in 2D geographic information systems, whereas knowledge of ore genesis is useful in the analysis and interpretation of mineral deposit exploration models in 3D. Geological modeling in 3D is important for understanding geological settings and metallogenesis and for targeting new mineral deposits (McCuaig and Hronsky, 2014).

Exploration models are divided into subjective and objective models based on the type of data used (Carranza, 2015). The subjective mineral ore exploration models use predefined and less flexible ore genetic theories whereas the objective models are based upon multiple geological observations. Data integration approaches in model development include these two types of models together and mutually use information from both ore genetic theory and geological observations in the delineation of promising areas for mineral exploration (Porwal and Carranza, 2015). These promising areas are typically known as intrinsic geological units (IGU) (Pan and Harris, 1992a). It is also called the intrinsic unit, because this feature is not detected through direct mineral deposit observations. The IGUs formally consists of some critical genetic factors (CGF) as necessary conditions for mineral deposit formation (Pan and Harris, 2000). The IGU was introduced as an evolution of intrinsic sample (IS) or sum of probable valuable geological areas (Pan and Harris, 1992b). An appropriately delineated IGU contains geological bodies that are genetically linked to the given mineral resource (Pan, 2010). The IGU proposal improves the methodology of target identification and delineation which, in turn, improves the results of mineral resource assessment. The IGU theory paved the way for a new platform to gather target identification attributes for mineral resource exploration (McCuaig et al., 2010).

The IGUs for a region consists of four major steps. In the first step, multiple geodata are used to establish the structure of the CGF and the recognition criteria for the deposit type of interest. In the second step, using the geological observations, occurrence probability values of the recognition criteria are estimated. In the third step, a synthesized occurrence probability is measured for each CGF. This probability is defined by an optimum linear combination of the probabilities estimated in the previous step. Finally, in the fourth step, the IGUs are delineated by optimally discretizing the probability values of the CGFs (Eberle et al., 2015).

The aim of this study was to construct a 3D geological model to visualize the intrinsic ore body and the hosting lithologies. Particularly, the model is for investigation of controlling structures on the deposit scale to determine the continuity of relevant geological units, including the ore zone, and to obtain a better understanding of the 3D structure and structural evolution of the ore district. Successful 3D modeling of exploration targets depends on recognition of the geological, geophysical, and geochemical criteria of a deposit model from relevant exploration datasets (Wang et al., 2015).

* Corresponding author.
E-mail address: b.jodeiri@hut.ac.ir (B. Jodeiri Shokri).

http://dx.doi.org/10.1016/j.oregeorev.2016.03.013
0169-1368/

In this study, a genetic deposit model was developed to facilitate chromite mineral exploration in the Sabzevar ophiolite region in NE Iran. After considering whether the exploration targeting criteria were representative, comprehensive, and accurate, we constructed geological objects in 3D space to model the existing knowledge of chromite metallogenesis in the Sabzevar district.

The main objective for establishment of this model was defining the CGFs, critical recognition criteria (CRC) and intrinsic parameters. These parameters were further used to create the conceptual genetic model (CGM) for chromite mineralization in the area. The CGM was developed based on the geological settings, geochemical and lithological properties of the mineralization zone and surrounding rocks and mineralogical analysis of the Sabzevar ophiolite lithological units. In addition to performing a full field data analysis, auxiliary data were collected from the results of previous studies in nearby areas, accompanied by construction of a medium scale information database of characteristics from similar mines around the world.

1.1. Petrogenesis and genetic models of podiform chromites

Alpine type chromite ore deposits comprise an integral part of the mantle sequences observed within many ophiolite complexes (Pagé and Barnes, 2009). Significant chromite deposits have been reported in the Philippines (Tertiary), Albania (Jurassic), Turkey (Jurassic–Cretaceous), and Kazakhstan (Silurian) along with the occurrence of many small deposits in the Caledonian–Appalachian orogeny (Kuno and Matsuo, 2000; Beqiraj et al., 2000; Parlak et al., 2002; Yiğit, 2009; Shafaii Moghadam et al., 2010a). Regarding the host rocks, almost all chromite pods are hosted by harzburgite and dunite rocks. In most of these samples, chromite ore bodies are bordered by dunite envelopes of variable thickness which show transitional boundaries to harzburgite host rocks (Shafaii Moghadam et al., 2013). Generally, podiform chromites in ophiolite sequences contain a large number of inclusions, such as silicates, sulphides, arsenide and fluid inclusions (Mondal et al., 2006; Proenza et al., 2001).

Several different hypotheses have been offered for the alpine type chromite genesis. Like the dunites to which they are clearly linked, chromite pods in ophiolite have been considered as magmatic cumulates settled at the base of the magma chamber (Gale et al., 2013). On the other hand, some other researchers proposed deposition by gravity settling in mantle 'mini-chambers', accumulation from the raising basaltic melt and tectonic insertion inside the peridotites (González-Jiménez et al., 2014). The later could explain various factors contribute in chromite and olivine crystallization including drop in temperature or increase in oxygen fugacity (Zabihi and Bozorgmanesh, 2014).

1.2. Geological setting

The geology of chromite deposits and the economic significance of the chromite producing regions of Iran have been discussed in several publications (Ghazi and Hssanipak, 1999; Ghazi et al., 1997; Hassanipak and Ghazi, 2000; Jannessary et al., 2012; Najafzadeh et al., 2008; Najafzadeh and Ahmadipour, 2014; Peighambari et al., 2016; Rahgoshay et al., 2006). Ophiolite complexes and colored mélanges in Iran have been divided into four settings and locations: (1) in northern Iran along the Alborz mountain range; (2) the Zagros suture zone, (3) the Makran region and (4) boundaries of the internal Iranian microcontinent (CIM) block, including the Sabzevar ophiolite (Fig. 1a) (Pournamdari et al., 2014).

The Sabzevar ophiolite is located between longitude 57 to 60° and latitude 33 to 37° in northeast Iran. The ophiolite builds up an east-west-trending mountain range approximately 200 km long with 3 to 22 km minimum and maximum widths, respectively (Fig. 1b). Fig. 2 illustrates the geological map of the study area. The three other boxes on the map show areas researched in other previous studies.

The Sabzevar ophiolite reveals a complete section typical of an ophiolite complex, with six exposures of ophiolite massifs (Shirzadi et al., 2013). In spite of being highly faulted and altered, the Sabzevar ophiolite is an example of outstanding ophiolites in Iran. It contains diverse types of igneous, metamorphic, sedimentary, hydrothermal and volcano–sedimentary rocks in different localities (Shafaii Moghadam et al., 2010b).

Results of previous studies reveal that this ophiolite is a small local branch of the Neotethys Ocean around the CIM in NE Iran. This branch was opened and closed during the late Cretaceous. Afterward, ophiolite complexes were formed as a ring structure around the boundary between the CIM and the Turanian Plate, as shown in Fig. 1a. The study area consists of small ophiolite zones belonging to the greater Sabzevar ophiolite sequence (Fig. 2). In this study, the northwestern part of the Sabzevar ophiolite complex was selected for genetic model construction. In the selected area, chromite disconnected lenses are scattered near the subsurface and are surrounded by the mafic and the ultramafic rocks. These country rocks are comprised of serpentinite, peridotite, dunite and harzburgite. The mantle rocks primarily consist of harzburgite and dunites, which are the principle rock types in the Sabzevar ophiolite (Shojaat, 1999). The sedimentary rocks of the complex consist of reddish pelagic fossiliferous limestone and radiolarian chert (Ghazi et al., 1997). The sharp lithological contacts between rock units are commonly faulted and highly tectonized. Chromite ore bodies usually occur within the dunite pockets inside the harzburgites (Hassan and Kassem, 2013). In the study area, the chromitite is always surrounded by an envelope of dunite, although this envelope can vary in thickness from less than 0.5 to several meters (Shojaat et al., 2003). Massive and nodular chromitites are occasionally stretched and appear as layers or as spindles due to their plastic deformation (Hassanipak et al., 1996; Rahgoshay et al., 2005).

1.3. Regional geology and petrology

Rock units of the Sabzevar ophiolite can be divided into ophiolitic and non-ophiolitic sequences. These groups, with different geologic units, are described in Fig. 1b.

1.3.1. Amphibolites and garnet amphibolites

The amphibolite and garnet amphibolite unit is likely the oldest basement of the area. It shows characteristic features of amphibolite faces, as produced by regional metamorphism. This type of amphibolites has been observed less frequently in the other ophiolitic zones in the CIM boundary. These rocks are sheeted in structure and have a gneiss banding texture (Ghazi et al., 1997).

1.3.2. Ultramafic associated rocks

Ultramafic rocks are widespread in the area and are known as the major lithology component acting as chromite host rock (Fig. 3). The overwhelming majority of rock types in this group are harzburgite and dunite, accompanied by lizardite, serpentinite, and pyroxenite (Fig. 3a, b).

Some outstanding outcrops of dunites are exposed in the southern part of the region, as large patches in harzburgite masses (Fig. 3c). Dunite rocks appear in patches that are dark brown, olive green, and often yellowish colored on the surface. However, they are strongly weathered, with poorly oriented veinlets on the surface (Fig. 3d). Lizardite and serpentinized lizardite occur at few localities and are not exposed as sharp units; rather, they only accompany other ultramafic rocks (Hassanipak and Ghazi, 2000). Serpentinites are highly oxidized and weathered in the area. In addition, they have slightly schistose texture and are light to dark green or brownish green, with deep reddish color in some parts of the area (Ghazi and Hssanipak, 1999).

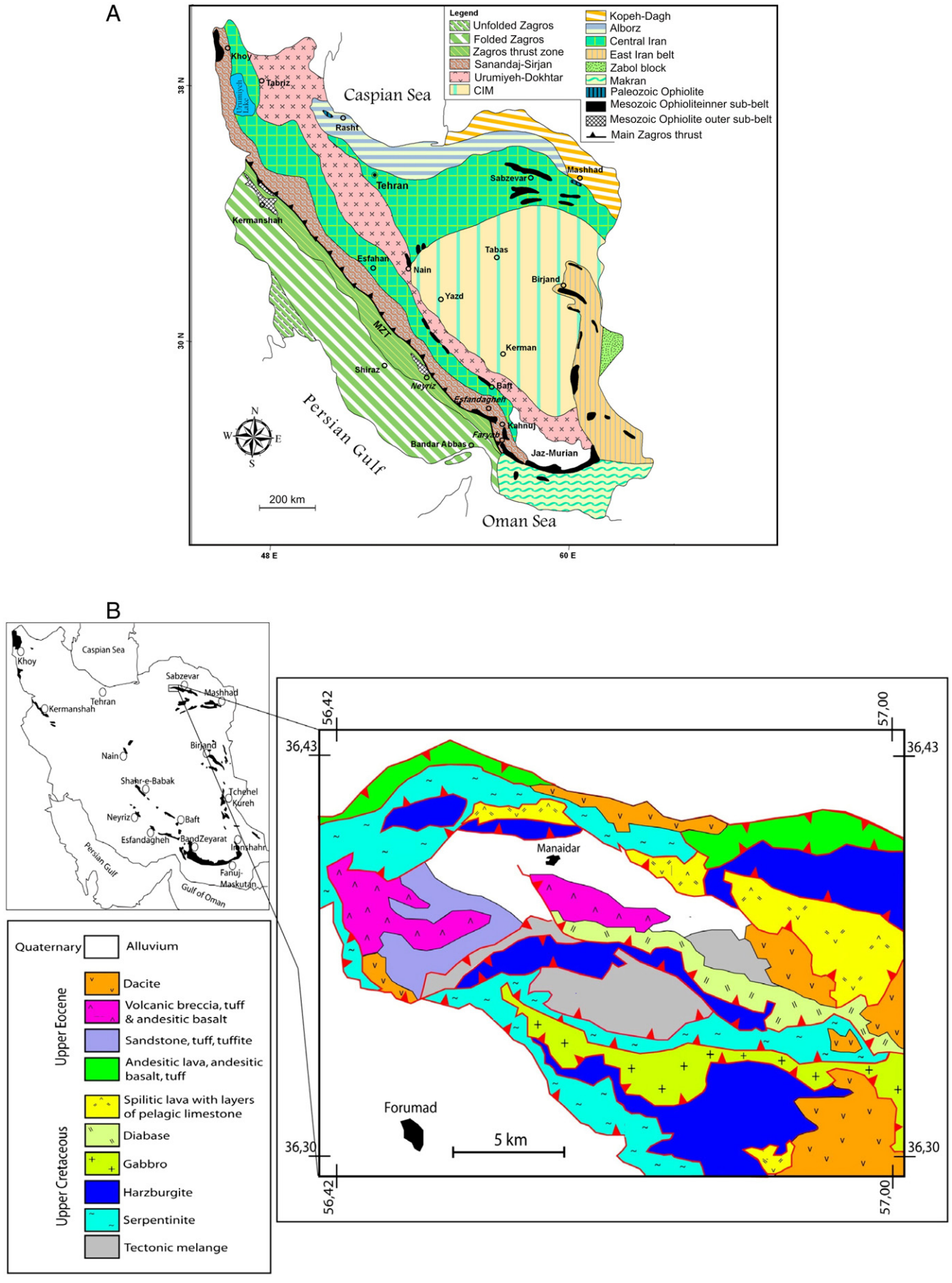

Fig. 1. (a) Iran geological zones and location of ophiolites and (b) Geological map of the area (Jannessary et al., 2012; Pournamdari et al., 2014).

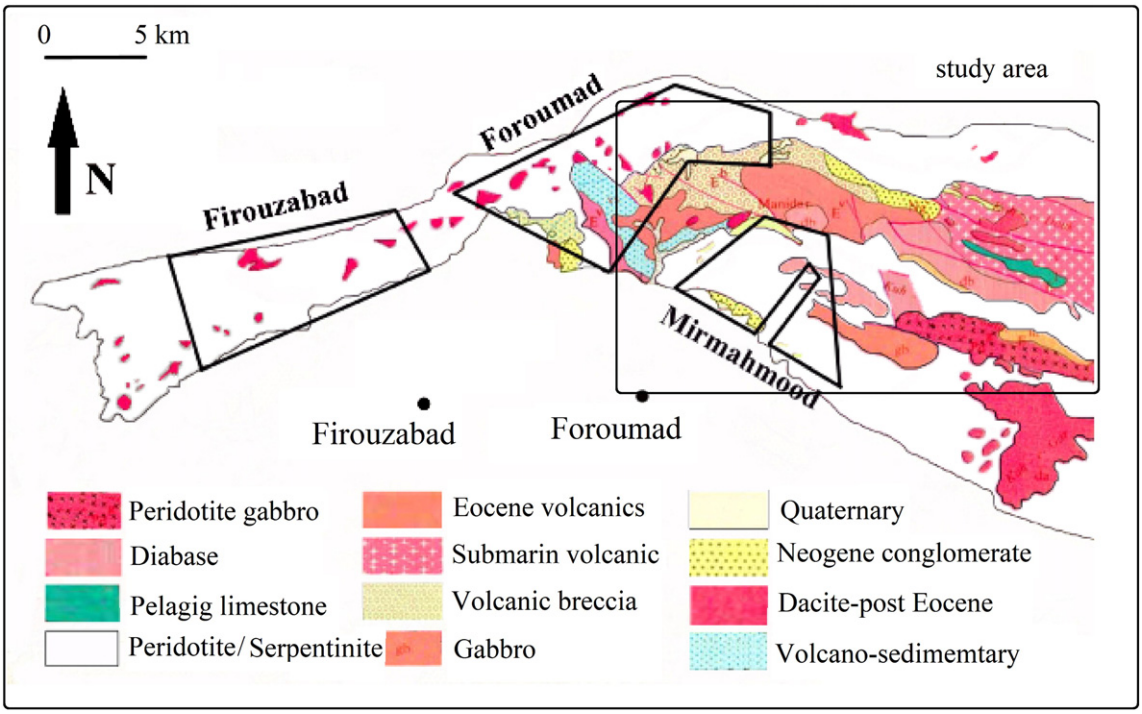

Fig. 2. Geological map of the area and other studied area by others used for comparison (Shirzadi et al., 2013).

1.3.3. Submarine lavas, tuffs and sediments

The second most significant and abundant constituent (after ultramafic units) in the Sabzevar ophiolite sequence is a lava-tuff series that has submarine facies with predominant pillow lava and hyaloclastite rocks. They are occasionally accompanied by pelagic limestone with shale and radiolarite (Roberts and Neary, 1993; Oki et al., 2012). They are fine grained micrites and are marly in some parts of the area.

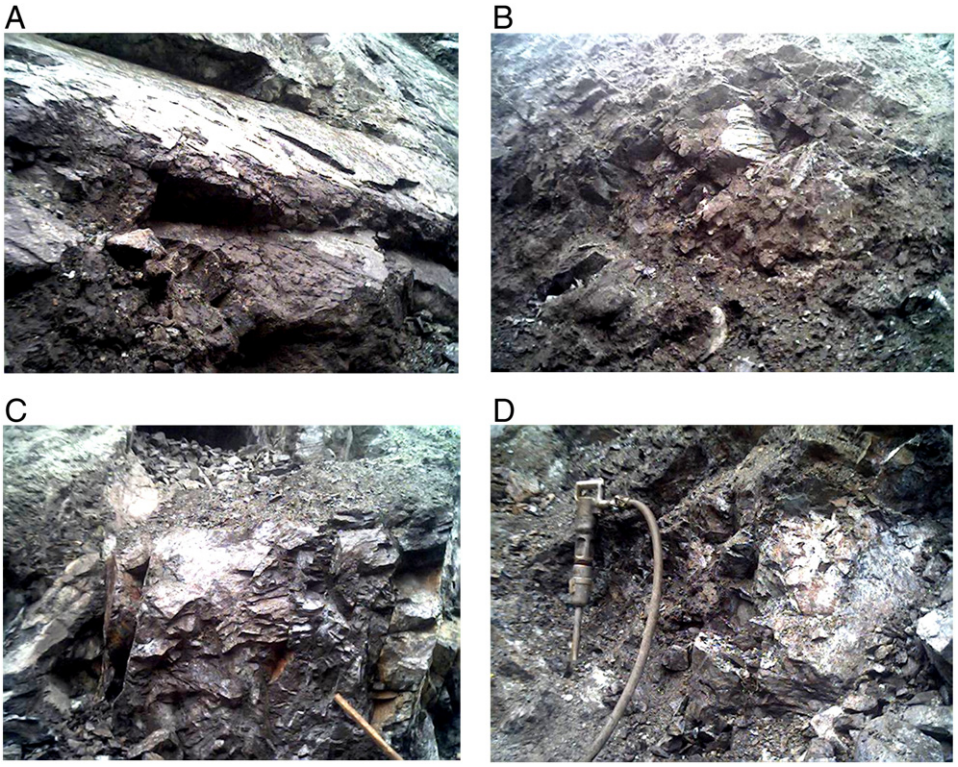

Fig. 3. Some photos from chromite pods in the area. (a) Chromite lenses are hosted by lherzolite and harzburgite. Thickness of lenses reaches 1 m in some mines in the area. (b) Pyroclastic sequence with chromite bearing ultramafic rocks. Widespread alteration is obvious in this image. (c) Ultramafic chromite bearing rocks. Most of them were altered to serpentinite with lizardite and antigurite type in dark green and creamy color. (d) A chromite lens hosted by the ultramafic rock, harzburgite.

2. Materials and methods

2.1. Geochemistry of the Sabzevar ophiolite

Thirty four samples from different igneous rock types were collected and analyzed by the X-ray diffraction (XRD) and the X-ray fluorescence (XRF) methods. Table 1 shows results of the XRD analysis on the rock samples. Results of the XRF analysis were applied to illustrate the rare earth elements (REE) which can be used for ore genesis modeling. As to the XRF analysis results, harzburgite is typically fresh and is characterized by its Mg# (Mg# = 100 × Mg2 +/[Mg2 + + · Fe2 +]) between 0.82 and 0.84.

The Mg# for harzburgite is slightly lower than those founded in the other ophiolites in Iran (Vatanpour et al., 2009; Yaghubpur and Hassannejad, 2006). This low Mg# is due to the lower Mg concentration in the harzburgite. The Mg# for gabbro is also slightly lower (0.50–0.62) than those from the other studied ophiolites in Iran (Yaghubpur, 2005).

The chondrite normalized REE patterns for different rock types of the entire sequence of ophiolite are shown in Fig. 4. The REE pattern in Fig. 4a, divides gabbro unites into two groups. Both these groups illustrate positive Eu anomaly, which is a characteristic of rocks with high modal plagioclase concentration. Basalts of the Sabzevar ophiolite show a similar pattern to the other ophiolite zones, with positive Eu anomaly and enrichment in light REE (LREE). Andesites and other extrusive rocks are also characterized by LREE enrichments (Shafaii Moghadam et al., 2009). While rhyolite is recognized by its negative Eu anomaly in the Sabzevar ophiolite sequence, rhyodacite–dacite rocks show a positive Eu anomaly in their pattern. This phenomenon can be attributed to the cumulative effects of plagioclase fractionation and to the removal of the Eu element during melting processes in a low oxygen fugacity (fo_2) environment (Rollinson, 2008). Overall, a steep dip near Nb in the REE pattern is a characteristic feature of extrusive rocks influenced by continental lithosphere in the volcanic arc environment (Paktunc, 1990). Meanwhile, rhyodacite–rhyolites are characterized here by a large Nb anomaly (Singh, 2008).

In addition to the major rock types mentioned above, additional rock types were also identified in the results of the geochemical analysis. The first group of these minor rocks is well-defined by high SiO_2 (67–97%) content and high Zr/Ti ratio. The second group shows characteristics of andesite rock with a wide range of SiO_2 concentration. The third group is related to basalt family with concentration of SiO_2 ranging from 22% to 41%. Finally, the last group is basanite with 40–44% of SiO_2. The Zr/TiO_2–Nb/Y diagram illustrates separation of different rock types in the Sabzevar ophiolite (Fig. 5).

The geochemical similarities between chromite in different parts of the study area imply that they should have the same origin in accumulation. Nevertheless, this deduction does not exclude the probable occurrence of other types of chromitites (e.g., tectonite) in this ophiolite.

The Al_2O_3 and TiO_2 contents of chromite are very useful to determine the nature of the parental melts of the chromitites and the tectonic setting of formation of these melts (Akmaz et al., 2014). Additionally, the Cr#, ($Cr\# = 100 \times Cr^{2+}/[Cr^{2+} + Fe^{2+}]$) and Fe^{+3} concentration of rock samples were also used as the most useful geochemical petrogenetic parameters for chromite genesis identification. Low observed concentration of Ti in rock samples suggests the mantle source for the parent magma. It is also in agreement with the Sabzevar oceanic lithosphere subduction scenario. The high Cr#, low TiO_2 and Al_2O_3 content of the parent magma is more consistent with boninitic melt produced by a sub-ducting oceanic lithosphere. Enrichment of Cr and more or less depletion of Al and Mg, which cause lower Mg# than expected for a boninitic melts, are probably due to penetrative hydrothermal processes, producing vast serpentinite masses in this ophiolite, or the result of subsolidus Mg–Fe exchange between Mg silicate and chromite after cooling.

2.2. Genetic deposit model

The genesis of podiform chromitites is not well understood and several models have been proposed to account for their formation. Fractional crystallization from a continuously supplied melt circulating through magmatic conduits has been considered as one of the main models (Najafzadeh and Ahmadipour, 2016).

Other processes such as multi-stage partial melting, magma segregation, melt/rock reaction, and magma mixing within the upper mantle may also be involved during magma generation (Rajabzadeh et al., 2013). Such models assume that melt/rock interaction and subsequently melt/melt mixing are the most important processes in the formation of podiform chromitites (Peighambari et al., 2016). In some cases, podiform chromite has a polygenetic origin, such as the Sikhoran mafic–ultramafic complex in central Iran (Ghasemi et al., 2002). More recently, melt–rock reaction has been proposed as the principal driver in chromite precipitation (Brough et al., 2015).

To enhance estimation of ore deposit occurrence probability in the host rock, one should consider the exploration model in conjunction with genetic, tectonic and other unifying geoscience models. As was previously stated, the chromite deposits in the Sabzevar ophiolite are in lens and lenticular shapes. They have massive nodular textures in dunite host rock. Sizes of the lenses vary from less than 1 m to tens of meters and the largest one of appears in the Gaft mine.

The most essential part of deriving an ore deposit genetic model is the initial construction of a complete database of the deposit characteristics information. Establishing a large database that contains information related to all mines from the entire world requires significant

Table 1
Minerals concentration in samples the analyzed by the XRD.

Sample. No.	Rock component mineral (%)						Chromite %
	Chamererite	*Magnetite*	*Serpentine*	*Clinopyroxene*	*Orthopyroxene*	*Forsterite*	
1	NA	NA	40	NA	Low	25	35
2	NA	NA	65	NA	Low	15	20
3	5	NA	25	10	Low	30	30
4	Low	NA	70	Low	Low	10	20
5	NA	NA	65	NA	Low	15	20
6	NA	NA	40	5	Low	30	35
7	NA	NA	45	Low	Low	30	35
8	10	15	35	Low	Low	30	NA
9	5	30	30	NA	NA	35	NA
10	15	NA	20	NA	NA	25	40
11	NA	NA	15	NA	Low	45	40
12	5	NA	40	5	NA	25	30
13	10	NA	40	Low	Low	25	30
14	NA	NA	70	Low	NA	15	15
15	NA	NA	65	Low	Low	20	10

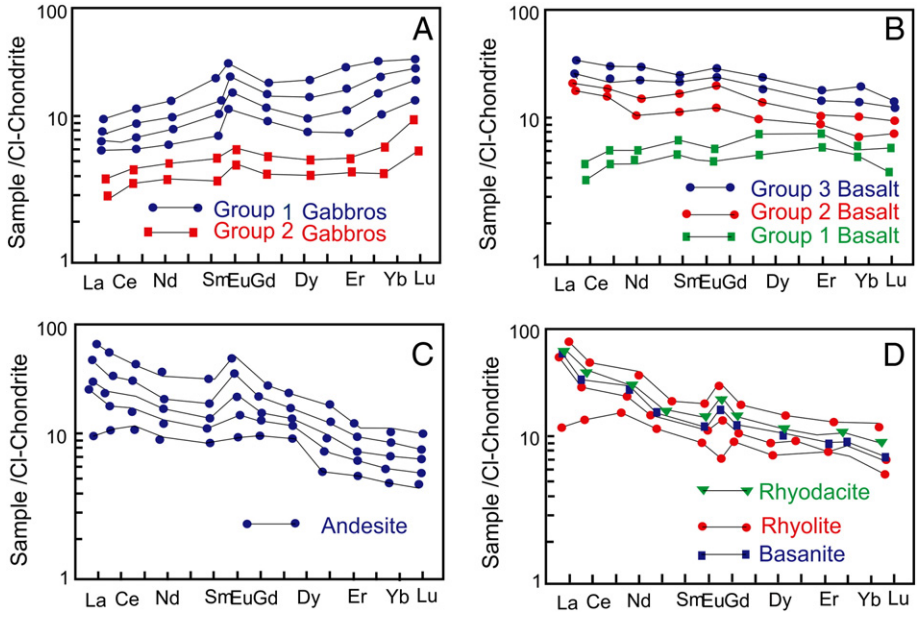

Fig. 4. Cl-Chondrite normalized REE patterns for all crustal rocks of the Sabzevar ophiolite. (a) This pattern divides gabbro into two units and (b) for basalt rocks into three groups. (c) Andesit shows enrichment in LREE and (d) shows different patterns of other rocks.

effort and time for appropriate classification of data. In this study, we have collected the required information to construct a medium scale database from different active mines or prospects from the entire world. Afterward, the geological and petrological data should be quantified for use in the model. Before describing the construction of the ore deposit genetic model, some geological concepts are explained below.

2.2.1. Intrinsic geological unit

The most traditional resource estimations have been made on the basis of regular inter-grids or cells as the sampling scheme and estimation unit. However, the conventional cell approach suffers from a number of drawbacks. The most significant problem is that geological processes can be reconstructed through observable geoscience features, which are measurable in geological units, not artificial cells (Pan, 1989). To resolve this problem in the cell approach, in contrast with a population of cells having multiple attributes, it is necessary to consider a population in which each number consists of a set of genetically related objects, for instance, igneous intrusive and associated altered rock. Each number in these cells is described by the field of the related geological objects. Here, mineral resource descriptors and geological

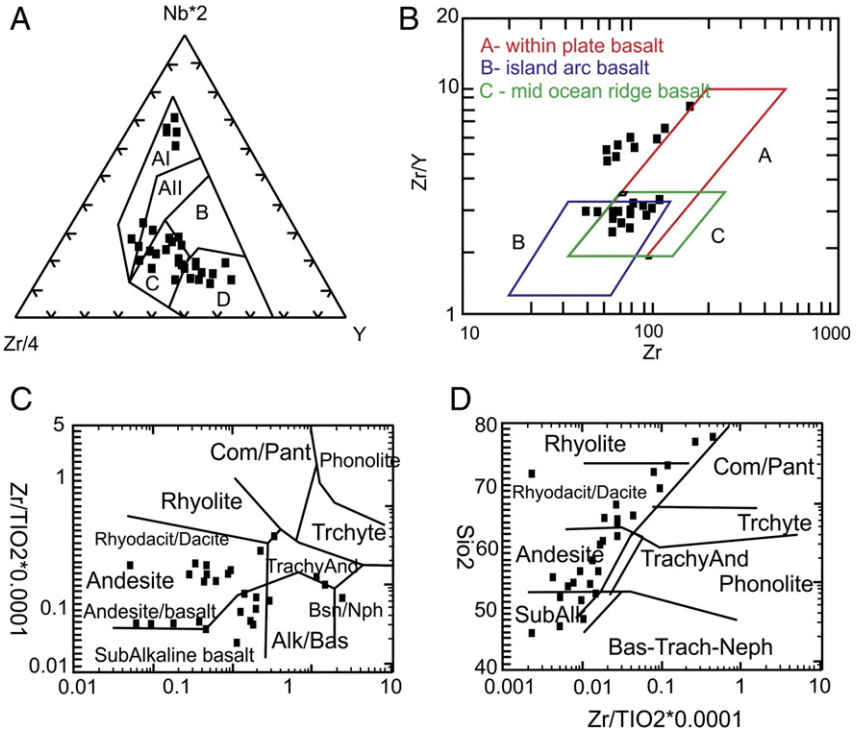

Fig. 5. (a) The Zr–Y–Nb diagram that shows distribution of the related extrusive rocks in the region; (b) The Zr–Zr/Y diagram shows different types of basalts; (c) The Zr/TiO_2–Nb/Y diagram and (d) the geochemical SiO_2–Zr/TiO_2 diagram shows identified rocks based on the result of geochemical analysis of the 34 samples.

evidences are attributes of a group of geological information which, in turn, are attributes of a set of genetically spatially related geologic bodies. Such a scheme was applied in a sampling reference for quantification and integration of geoscience information that is intrinsic to the deposit type being sought. Areas with such populations are defined as the IGU. The IGU can be described as members of a population consisting of sets of genetically related geologic objects that are usually defined by their geo-fields (Harris and Pan, 1990). Both time and spatial factors (in the area) should be considered in deriving a genetic model. In other words, the IGU is a link between the evidence obtained by field observations and analysis in time factor and a connection between prospecting and detailed exploration criteria, in spatial factor. In this study, "time factor" in model generation refers to the sequence of exploration activities and data analysis as to the sequential occurrence of mineralization events.

2.2.2. Critical genetic factor

A genetic model consists of a hierarchy of earth processes, from preconditioning to post mineralization preservation process, which acted during one or more previous time periods. However, a number of necessary conditions may exist for a particular genetic process or mineralization, and in all of the cases, one or at most a few of them are referred to as critical (Afzal et al., 2016). These conditions are called critical genetic factors (CGF). A linear combination of these parameters would give a function that is responsible for IGU generation. If one of these CGFs is not present, the IGU is considered to be absent.

In geologically simple mineral deposits, *i.e.*, deposits with less than three ore minerals or deposits in simple structures, there are typically not many effective geological events affecting the mineralization. In such deposits, the relationship between effective mineralization events is also simple and can be demonstrated by linear functions in defining the CGFs (Li et al., 2016). However, it is not the case in most of the complex deposits, *i.e.*, deposits with more than three ore minerals or deposits in complex geological structures. Alpine chromite deposits are not as simple as its layered counterpart but also not as complex as other ore complex deposits. Therefore, using a linear function of CGF parameters to produce IGUs would be feasible for this type of deposits.

2.2.3. Critical recognition criteria (CRC)

A set of special geological features that indicate the existence of the CGF have to be obtained before one can use the CGFs for IGU definition. Such features are called the critical recognition criteria, (CRC). For instance, in a hydrothermal deposit model, the alteration process is considered as the CGF, where its related CRCs are the altered minerals found in the rock samples. If the CRCs are considered as terms of a function, due to their accumulative properties, their presence in a special location will give high scores in producing the IGU in that part. Table 2 shows the CRCs used for IGU establishment in this study for alpine type chromite deposits. Scores for each CRC are presented in the target and the exploration functions. These scores are based on the information obtained from the previously constructed characteristics information database (Table 3) (Elipoulolos and Vacondios, 1995; Schiano and Masser, 1997; Happel et al., 1998; Billor and Gibb, 2001; Hofer et al., 2001; Ghasemi et al., 2002; Becque et al., 2003; Hariri, 2004; Rahgoshay et al., 2006; Yiğit, 2009; Chandrasekhar et al., 2009; Hashim and Pournamdary, 2011; Uysal et al., 2009; Pournamdari and Hashim, 2013; Kop et al., 2014). In Table 2, an NA (Not Applicable) cell reveals that the related geoscience field is not applicable as an exploration tool for that type of deposit. However, it should be noted that an NA cell in the exploratory function depicts a not applicable geoscience field in regional exploration. Meanwhile, an NA cell in the target function indicates a not applicable parameter in detailed exploration. For instance, "electric" which is NA in both columns, means that the electric method is not applicable for either regional or detailed exploration for alpine type chromite deposits.

Table 2
Target and explanatory geological variables for alpine type Chromite deposit.

Geoscience fields	Target function	Explanatory function
Geological		
Host rock	+++++	+++++
Pre-mineralization units	++	+++
Post-mineralization units	++++	+++
Regional structures	+	+
Local structures	+	++
Hydrothermal alteration	++	+++
Mineralogy	+++	+++++
Mineral occurrences	+++++	+++++
Deposit genetic models	+++	+++++
Geochemical		
Main element	+++++	NA
Indicator element	+++	+++++
Associate element	+	+++
Geophysical		
Magnetic	++++	+++++
Gravity	+++	+++++
Electromagnetic	NA	NA
Electric	NA	NA
Remote sensing		
Structural mapping	++	+++++
Alteration mapping	+++	+++++
Geological mapping	+++++	+++++
Topographic		
Elevation models	+	+++

+++++ Strong, +++ Moderate, + Weak, NA: Not Applicable.

The geoscience field parameter, *i.e.*, "main element", indicates a different concept. Observing the main element in any exploration activity gives the highest confidence in finding the target. However, it does not hold within all mineral exploration activities. For instance, gold minerals could hardly ever be observed in gold mineralization zone exploration, but it is not the case for iron exploration activities. This issue not only relates to different mineral ores but also to different exploration steps. For alpine type chromite exploration, in the initial steps of regional exploration, chromite mineral might not be observed directly as the main element. So it deserves low scores in the first steps of exploration. However, in case of "Target Function", the main element is exactly what we are searching for. It should be noted that function scores in Table 2 are applicable for alpine type chromite deposit exploration only, not generally for other chromite deposit types.

2.2.4. Model generation

The 3D geological models are built step by step based by field geological observations, in conjunction with geochemical, petrological, and mineralogical data. The procedures for 3D modeling and integration of spatial features for generation of exploration targets involve three stages: (1) 3D geological modeling for understanding the geological setting; (2) 3D modeling of large chromite deposits for understanding the ore-forming controls and metallogenesis and (3) 3D modeling and extraction of features representing exploration targeting criteria using various datasets.

The IGU concept is used as an exploratory tool to improve target identification and delineation strategy, and in turn, for improving the efficiency of mineral resource exploration in the Sabzevar ophiolite. The IGU theory creates a new platform on which new approaches to mineral target identification can be constructed. To emphasize the IGU target identification ability, the relation between the IGU and the mineral target should be clarified.

To state this relevance, suppose the function Φ denotes a mineral resource descriptor (*e.g.* mineralization). Assume that the study region (A) contains only a single intrinsic geological unit (U). Now consider target variables Y_1, Y_2, Y_3,..., Y_τ, (*e.g.*, indicator minerals, alteration, fault density, and geophysical response) as geological evidence

Table 3
A sample of information database of alpine chromite deposits (Elipoulolos and Vacondios, 1995; Schiano and Masser, 1997; Happel et al., 1998; Billor and Gibb, 2001; Hofer et al., 2001; Ghasemi et al., 2002; Becque et al., 2003; Hariri, 2004; Rahgoshay et al., 2006; Yiğit, 2009; Chandrasekhar et al., 2009; Hashim and Pournamdary, 2011; Uysal et al., 2009; Pournamdari and Hashim, 2013; Kop et al., 2014).

CRC	Gaft & Soror (Iran, Case study)	Esphandagheh &Faryab (Iran)	Cobb Intrusive (New Zealand)	Pindos Mine (Greece)	Kizildag, Hatay,Islahiye (Turkey)	La cabana Mine (Chili)	Tiebaghi (New Caledonia)	Jabal Zalm (Saudi Arabia)	Moa Mine (Cuba)
Host rock (dunite & Harzburgite)	Dunite & Harzburgite	Peridotite rocks (dunite)	Dunite & Harzburgite, Serpentinite	Dunite & Harzburgite	Dunite, lherzolite and transition zone	Dunitic rocks	Dunite, lherzolite	layered gabbro	Peridtite rocks (dunite)
Associated minerals	Chrysotile, magnetite, lizardite	Chrysotile, chlorite, chamererite	Fuchsite, magnetite, vesouvianite	Chrysotile, chlorite, chalchophile elements	Chrysotile, chlorite, Cu and Ni solfide	Vesouvianite, chlorite, fuchsite, chrysotile	Magnetite, chlorite	antigorite and chrysotile	chrysotile, chlorite, Zoasite, Yovarovite
Dunitic dyke In the region	–	–	Less dunitic dyke & pyroxenitic	–	Dunitic & pyroxenitic dyke	–	–	–	Dunitic dyke
Alteration and weathering	Large serpentinization	Many serpentinized vein	Large serpentinization	Large serpentinization	Local alteration	Chromite to ferric chromite	White serpentinized dunite zone	Large serpentinization	Chamererite to oxidized laterite limonite
texture	Nodular & disseminated	Nodular & massive	Nodular & less disseminated	Nodular & disseminated	Nodular & disseminated, massive	Nodular & disseminated	Nodular	disseminated	Nodular & disseminated
Overlapping with airmag map	Good	Good	Not good	–	–	Good	Little	Good	Good
#Mg and #Cr	0.72# > Cr 0.84# < Mg	–	0.8# < Cr	–	0.81# < Cr < 0.72 0.75# < Mg < 0.72	0.6# > Cr	–	–	0.75# < Mg 0.7# > Cr
Depletion of TiO_2 and negative Nb anomaly	Less TiO_2 & negative Nb anomaly	TiO_2<	TiO_2<	$TiO_2 < 0.1$	$TiO_2 < 0.2$ — Nb anomaly	<TiO_2 & — Nb anomaly	–	–	–

pertaining to the mineralization of interest, Φ. As in a geologically simple deposit model, this relevance can be stated by a linear combination as follows (Pan and Harris, 2000):

$$\Phi = \beta_1 Y_1 + \beta_2 Y_2 + \beta_3 Y_3 + \ldots + \beta_t Y_t \tag{1}$$

where β_i is a known coefficient of the geological evidence. According to Eq. (1), the mean and the variance of Φ can be estimated as follows (Pan and Harris, 2000):

$$E(\Phi) = \sum_{i=1}^{t} \beta_i E(Y_i) \tag{2}$$

$$Var(\Phi) = \sum_{i=1}^{t}\sum_{j=1}^{t} \beta_i \beta_j COV[Y_i, Y_j] \tag{3}$$

In general, the spatial nature of the target can be described by the probability distribution of Φ or probabilities transformed from its favorability index (Pan and Harris, 1992b):

$$F(Y_1, Y_2, Y_3, \ldots, Y_t, y_1, y_2, y_3, \ldots, y_t) = \mathrm{Prob}\{Y_1 < y_1, Y_2 < y_2, Y_3 < y_3, \ldots, Y_t < y_t\} \tag{4}$$

Where $y_1, y_2, y_3, \ldots, y_t$ are cut-off values that define thresholds for target variables. Any value for target variables below these thresholds will reduce the presence probability of Φ. However, for any set of cutoff values, $y_1, y_2, y_3, \ldots, y_\tau$, a corresponding value for the mineral resource descriptor Φ can be calculated by the following equation (Pan and Harris, 1992b):

$$\Phi = \beta_1 y_1 + \beta_2 y_2 + \beta_3 y_3 + \ldots + \beta_t y_t \tag{5}$$

Accordingly, the probability function of Φ can be expressed in terms of joint probability function, F, of (Y_1, Y_2, Y_3,…, Y_τ):

$$\Phi_p = F_\phi^{-1}(P) \tag{6}$$

Where Φ_p is the probability value for the mineralization of interest and F_Φ is the probability function for Φ. Now, suppose that the whole study area is subdivided into small units of equal volume, with each unit centered at location X (x_i, y_i, z_i) in 3D Cartesian coordinates. A point (location) set denoted by Ω for all points within the IGU of the study area, containing unit blocks centered at the points in Ω is defined as (Pan and Harris, 2000):

$$U = \{u_x : x \in \Omega \in A\} \tag{7}$$

This is exactly the desired IGU. Membership of each point X (x_i, y_i, z_i) in Ω is defined by Pan and Harris (2000):

$$\Delta\phi = \left\{x : \phi > \phi_p, x \in \Omega\right\} \tag{8}$$

Where Δ is a function of Φ. Moreover, by definition of the following volume set:

$$V_\phi = \{V_x : x \in \Delta(\phi)\} \tag{9}$$

Where V_Φ is referred to as the target of Φ, the final relation is as follows (Pan and Harris, 1992b):

$$V_\phi \subseteq U \subseteq A \tag{10}$$

The above relation is sketched in Fig. 6 as a hydrothermal mineralization example.

It is important to note that “ore body” by itself is not a well-defined unit in such models (Saalmann and Laine, 2014). It is generally not

stated whether the ore body represents a specific area as the target or if the mineral enriched zone is the unit of interest. There are different to describe the rating of each alternative and the weight of each criterion in linguistic terms, which can also be expressed in triangular fuzzy numbers. In the above equations, the points with $Y_i > y_i$ are referred to as U, and the minimum value for y_i is called the threshold. Definitions of these values for each type of mineralization should be carried out separately. To perform this definition, an information database of alpine type chromite deposit is needed. This database was constructed previously and a small sample of it is shown in Table 3.

3. Results and discussion

3.1. IGU definition for Sabzevar chromite pods

The main objective of this model is to define CGF, CRC and intrinsic parameters to generate the conceptual genetic model (CGM) for chromite mineralization in the area. This model can also be used to define a method for quantifying spatial associations between known mineral deposits and effective layers in mineralization. These quantified parameters are later used as inputs for geologically constrained predictive mapping of prospective minerals. The principal steps of the CGM creation for IGU definition are illustrated in Fig. 7. In this strategy, the CRCs are arranged in a matrix format in the model. In this matrix, the rows and columns are populated with the CRCs and chromite mine data, respectively (Table 4).

We used simple binary scoring in Table 4. Although fuzzy scoring is used in some genetic model generation studies, this type of scoring is not fully understood for alpine type mineralization parameters. Thus, it might introduce unknown artifacts into the model. Thus, we decided to use binary scoring in order to prevent any unknown distortion in the final model.

There were two rows in Table 4 with a 1 score for all the chromite mines, the “associated minerals” and “alteration and serpentinization” rows. Associated minerals are the results of alteration and serpentinization; because the associated minerals are result of alteration, these two parameters are internally related. However, this is not the case for all types of alteration and, above all, not for alpine type chromite deposits. Different alteration procedures produce different associated minerals. Although the values of these two parameters are quall to one for all mines, the minerals are different in different mines; thus, this difference was previously taken into account in Table 3.

Values of arrays in the matrix were one for mines having that particular CRC and zero for mines without it. After defining the CGM, the selected criterion should be applied to the IGU description. This process is described in Fig. 8. It should be noted that only shallow chromite pods were considered in model generation. Due to the low production rate and small size of the chromite pods in the Sabzevar region, economic benefit rapidly decreases as the pods emplacement depth increases. These pods are also located above a complex petrological unit called the colored mélange. Thus, in increasing the exploration depth, the geological complexity also increases, dramatically complicating the relationship between CGFs and IGU. Thus we adhered to the study of shallow depth chromite pods in our model generation strategy.

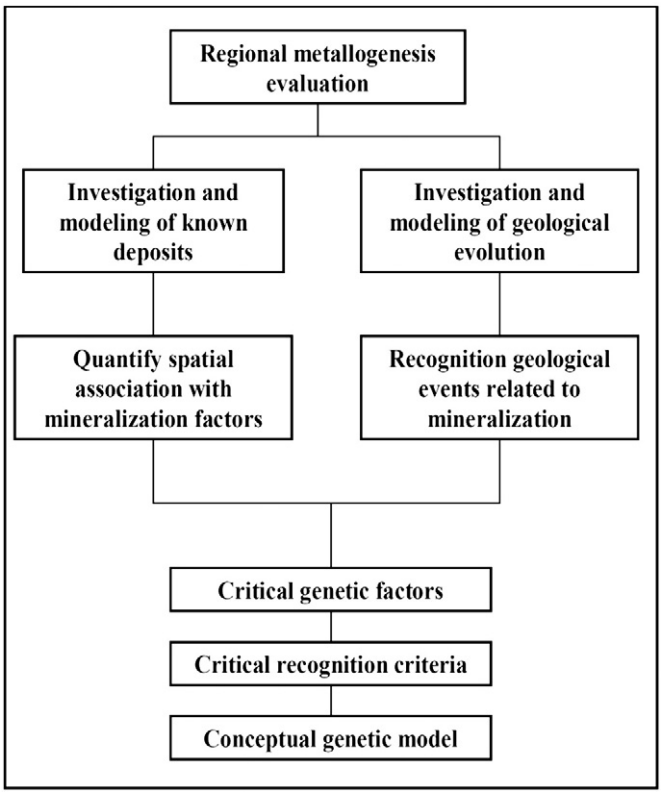

Fig. 7. A conceptual genetic mode preparation of the CGM (Chandrasekhar et al., 2009).

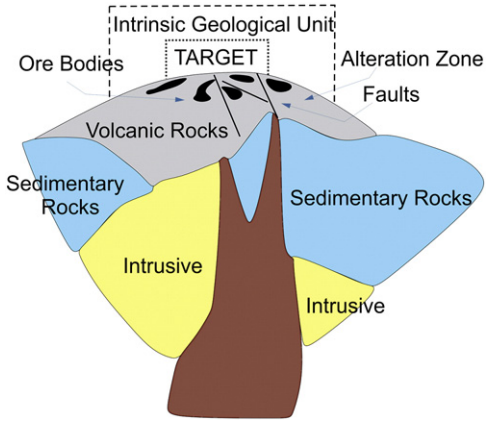

Fig. 6. A conceptual model of intrinsic geological unit in a hydrothermal example (Pan and Harris, 2000).

3.2. Discussion of the IGU model

Multiplying the CRC matrix into its transposed results in a matrix of characteristics. Subsequently, the sum of the second square root of values for each row was calculated. The final result was a matrix with one column of its arrays representing the value of each CRC. Arrays in each row of the last matrix show the weight of each parameter through the model representation. Afterwards, the CRCs were sorted from the highest to the lowest values for better identification. The highest weight (here, the host rock) is the first parameter that should be taken into account in the exploration outline.

At a known location, (with at least one observed CRC), the probability of CGF should be one or very close to one. This implies that the selected point is almost surely within the IGU. At an unknown location (with no observed CRCs), all of the CRCs probabilities are estimated from geoscience data, which will provide a measure of chance of the presence of the CGF. Presence of a specific CRC provides available evidence for the existence of an IGU. Boundary delineation of the IGU is obviously controlled by the resolution of the geoscience field observations associated with the CRCs.

For alpine type chromite deposits, we proposed that only spaces (geological units) with more than 75% of the CRCs comprised the IGU in the model. Geological units that contain between 50–75% of the CRCs are determined to be regions with mineral potential, indeterminate for further exploration decisions. The geological units which contain between 25% and 50% of the CRCs are regions in which any

Table 4
Matrix shown the values allocated to different properties of chromite deposits in different countries (Names of the mines are listed in Table 3).

	Turkey Mines	Philippine Mines	Chile Mines	Greece Mines	NZ Mines	Cuba Mines	Saudi Arabia	Iran Mines
Host Rock (Dunite & Harzburgite)	1	1	1	1	1	1	0	1
Associated minerals (Antigorite, Chlorite)	1	1	1	1	1	1	1	1
Dunitic Dyke	1	0	1	0	0	1	0	0
Alteration and Serpentinization	1	1	1	1	1	1	1	1
Texture	1	0	1	1	0	0	1	1
Overlapping with air-mag map	1	0	1	0	0	1	0	1

exploration activity should be undertaken with care. Finally, the geological units with less than 25% of the CRCs are considered to be barren regions.

However, it should be noted that for any prospect, there is no region containing all 100% of the CRCs. This classification is shown in Table 5. Estimation of the probability in areas with a low number of the CRCs is somehow controversial. In the other words, low numbers of CRCs do not sustain their use in geostatistical methods. Here, we used a simple conventional estimator function in areas with low evidence of CRCs.

Fig. 9 shows the IGU defined in the surface of the Sabzevar ophiolite complex. The area shows a surface with CRCs values above 75%. The final 3-D model that could be used for further exploration decisions, (CRC values above 75%) is shown in Fig. 10. Meanwhile, Fig. 11 shows only the IGUs with CRCs above 90%. According to the CRCs classification in Table 5, these units are proposed for drilling activity. It should be noted that chromite lenses in the Sabzevar ophiolite are small in size relative to the chromite pods in mines from other countries. Therefore, the IGUs with CRCs above 90% would be rather small in size, too.

The classification used in Table 5 is based on the probability of success in target exploration according to geological concepts. It is a qualitative and semi-quantitative classification, and as such, no mathematical equations were used to create this table. Therefore, selection of these thresholds is related to the chance of success in different units. Due to the size of the chromite pods in the Sabzevar ophiolite and the high cost of drilling in an area with such rugged topography, the proposed areas for drilling should have high probability of success. It is clear that proposing the areas above 80% may give a larger area, but it reduces the chances of success. Hence, we proposed areas above 90% for drilling and areas between 75–90% for further activities.

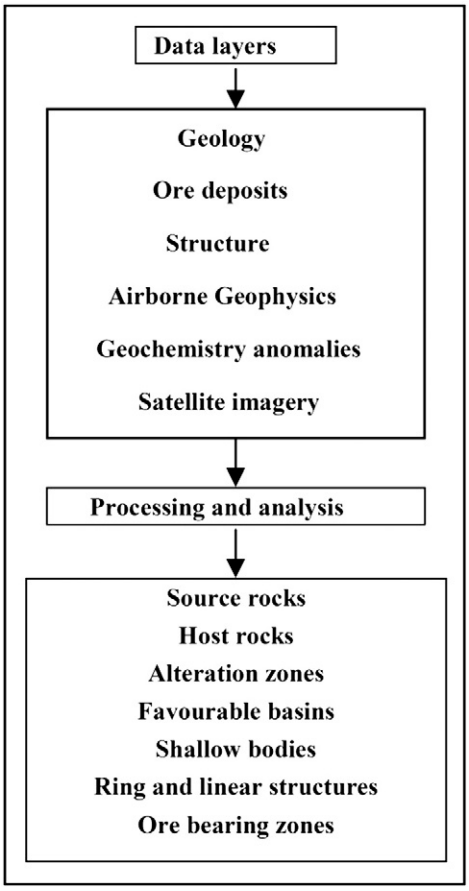

Fig. 8. The IGU model generation by the selected CRCs and CGFs.

Nonetheless, further exploration activities, especially drilling, should be undertaken to prove precision of the model. Accuracy of the model could be evaluated by other exploration activities such as geophysical methods. This evaluation has been performed by other researchers. Because of the complexity of the mineralization and polyphase deformation and remobilization of the ore, several deposit models have been proposed for the chromite ore in the Sabzevar region. However, detailed review of their results, combined with new geochemical analysis carried out during the study, led to the reinterpretation and presentation of the proposed petrogenesis model for the Sabzevar ophiolite presented here.

To examine the results of the previous petrological study, the chromite deposits were separated into highly Cr rich (especially in Gaft and Forumad areas) and less Cr-rich (in Kuh-siah area, the same area as in this study). In the Forumad area, there were huge chromite deposits, undoubtedly preserved by thick dunite integument within depleted harzburgites. Massive to nodular chromitites are dispersed in the altered dunite bodies. Nodular chromites show spindle form, due to the mantle plastic deformation. The Cr_2O_3 content of these chromites varies between 58 and 60 wt%, while Al_2O_3 content is approximately 10 ± 1 wt%. In the Kuh-siah area (North of Sabzevar) some small chromite pods with dunite cortex are associated with inter-fingered dunites, harzburgites and lherzolites.

Through comparison of the Kuh-siah chromites with the Forumad ones, it appears that melting is responsible for formation of the Frumad chromites, characterized by picritic composition, while for the Kuh-siah chromites, chromite bearing magma shows tholeiitic basalt behavior. These parameters for IGU definition and exploratory target definition were reported in massive chromite bodies hosted in the Veria ophiolite in northern Greece and in dunite from the slow-spreading southwest Indian Ridge (Morishita et al., 2007; Moutte, 2006; González-Jiménez et al., 2011). These observations were all observed in areas selected by the model as IGUs, shown in Figs. 10 and 11.

4. Conclusions

The significance of chromite has inspired many geologists to investigate its genesis and natural distribution as an important

Table 5
Area classification by CRC values.

CRC value (%)	Proposed considerations for exploration activity
90–100	High probability of mineralization occurrence
75–90	IGUs, proposed for exploratory investment
50–75	Region with mineral potential, not so good and not so bad for further exploration
25–50	Any exploration activity should be carried out with care.
0–25	Barren regions

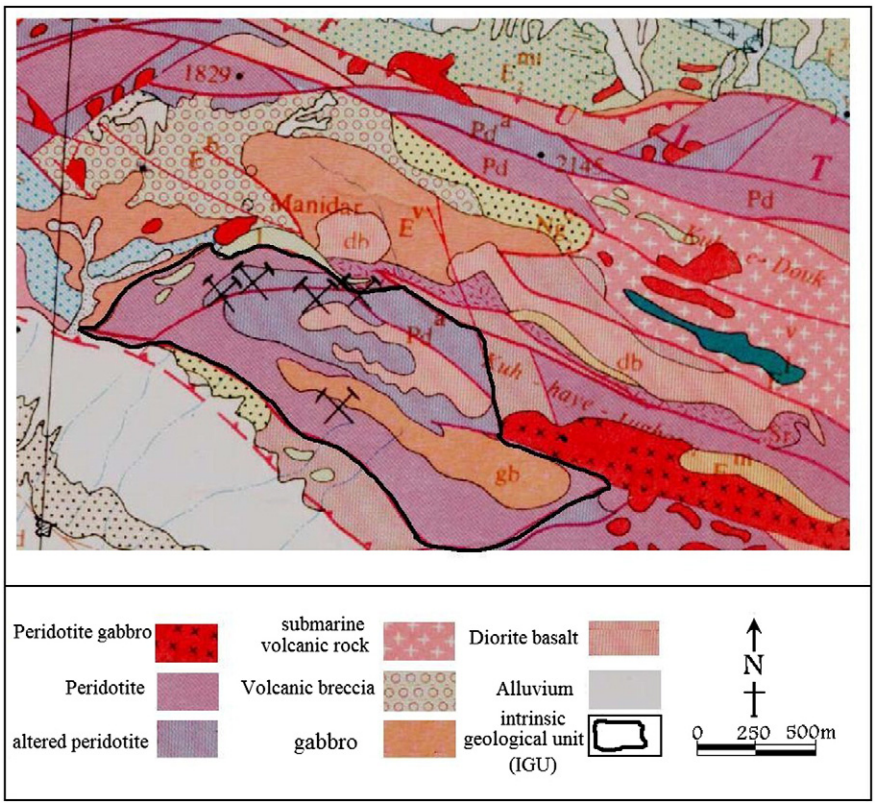

Fig. 9. The IGU defined by deriving the genetic model and the CRCs for chromite pods of the region.

contribution to its exploration. Thus, the geochemistry of chromite is considered to be a reflection of the nature of its parent magma and its geological settings have been extensively studied by many researchers. The chemical composition of chromium bearing minerals has been used as a petrogenetic indicator and as one of the key parameters for genetic model generation. In the Sabzevar region, based on the constructed characteristics information database, geochemical study of the rock samples and nature of the chromite parent magma, the related CGFs and CRCs were defined for delineation of the CGM. Rock samples containing the chromite ore showed high Cr# (86–88), moderate Mg# (44–51) and low TiO_2 content (0.1–0.2 wt%). According to the results of previous research, petrography and geochemistry projects, and field observations presented in this study, the chromitites must be generated in a supra-subduction zone setting. It appears that sea floor hydrothermal processes probably caused the Mg# to be lower than expected. The main mass of the Sabzevar ophiolite is composed of mantle rock consisting of harzburgite, dunite and serpentinite. Pyroxenite and isolated zones of olivine–chrome spinel cumulates are less abundant and form dikes or other small intrusive bodies. The crustal igneous rocks are gabbro, diabase sheeted dikes, pillow and massive basalts, and several groups of intermediate and acidic igneous rocks.

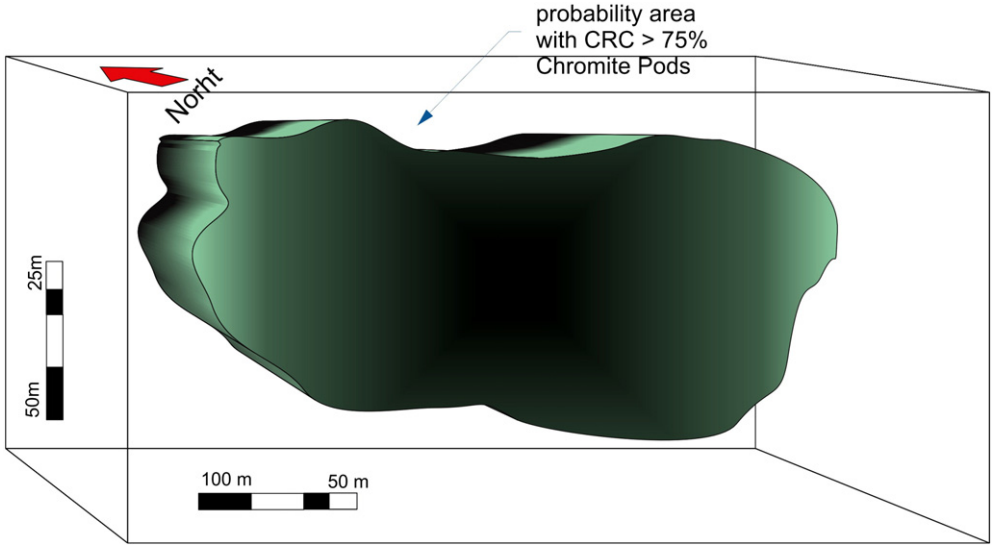

Fig. 10. The 3D IGU model for the Sabzevar ophiolite defined by deriving the genetic model and the CRCs values above 75% for chromite pods of the region.

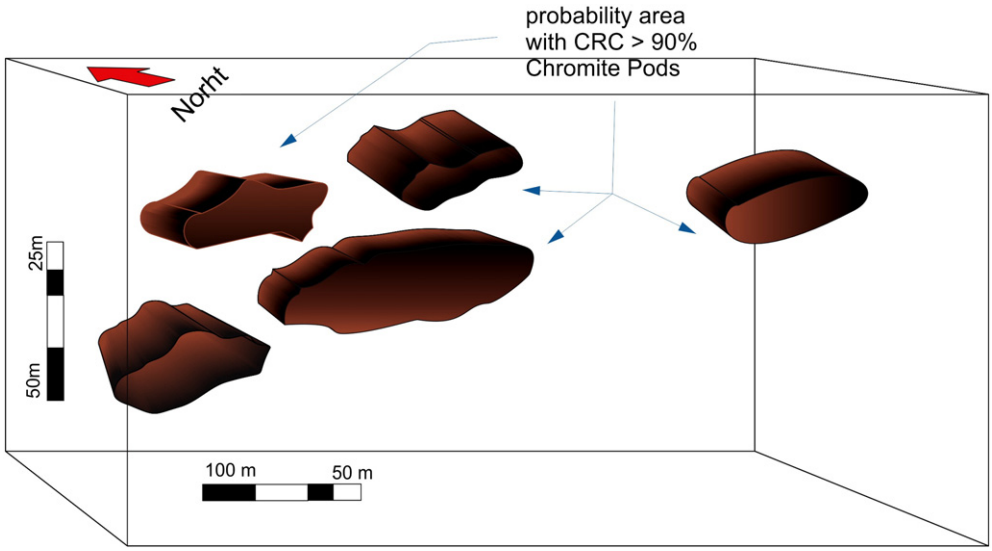

Fig. 11. The 3D IGU model for the Sabzevar ophiolite defined by deriving the genetic model and the CRCs values above 90% for chromite pods of the region.

Through application of the model obtained by incorporating the above mentioned information on the Sabzevar ophiolite, the top CRCs can be listed as follows:

- Harzburgite and dunite are known as the principle host rock and the principle component of the ophiolite sequence.
- Chrysotile, lizardite and chlorite are CRCs as associated minerals.
- High-level serpentinization and its resulting minerals such as magnetite and hydro-magnesite were observed in IGUs.
- The Mg# varies between 0.82 and 0.84 in harzburgite.
- Negative anomaly of Nb and depletion of TiO_2 were observed.
- High relevancy between mineralization in the IGU and magnetic anomalies.

The IGUs that were obtained using the method introduced here contained almost all of the above mentioned CRCs. Therefore, it could be concluded that the CGMs derived here for the Sabzevar chromite pods could define the areas that are considered to be favorable for drilling. The 3D model representing different CRC levels reveals that the small scale structural geometry of the ore bodies mirrors their petrogenesis evolution and vice versa, facilitating a program of further drilling.

References

Afzal, P., Eskandarnejad, M., Ghaderid, M., Hosseinid, M.R., 2016. Delineation of supergene enrichment, hypogene and oxidation zones utilizing staged factor analysis and fractal modeling in Takht-e-Gonbad porphyry deposit, SE Iran. J. Geochem. Explor. 161, 119–127. http://dx.doi.org/10.1016/j.gexplo.2015.12.001.

Akmaz, R.M., Uysal, I., Saka, S., 2014. Compositional variations of chromite and solid inclusions in ophiolitic chromitites from the southeastern Turkey: implications for chromitite genesis. Ore Geol. Rev. 58, 208–224. http://dx.doi.org/10.1016/j.oregeorev.2013.11.007.

Becque, T., Quantin, C., Sicot, M., Boudot, J.P., 2003. Chromium availability in ultramafic soils from New Caledonia. Sci. Total Environ. 301, 251–261. http://dx.doi.org/10.1016/S0048-9697(02)00298-X.

Beqiraj, A., Masi, U., Violo, M., 2000. Geochemical characterization of podiform chromite ores from the ultramafic massif of Bulqiza (eastern ophiolite belt, Albania) and hints for exploration. Explor. Min. Geol. 9, 149–156. http://dx.doi.org/10.2113/0090149.

Billor, M.Z., Gibb, F., 2001. The mineralogy and chemistry of the chromites deposits of southern (Kizildag, Hatay and Islahiye) and Tauric Ophiolite Belt (Pozanti–Karsanti), Turkey. Geological Survey of Turkey, Open File Report, pp. 1061–1074.

Brough, C.P., Prichard, H.M., Neary, C.R., Fisher, P.C., McDonald, I., 2015. Geochemical variations within podiform chromitite deposits in the Shetland ophiolite: implications for petrogenesis and PGE concentration. Econ. Geol. 110, 187–208. http://dx.doi.org/10.2113/econgeo.110.1.187.

Carranza, E.J.M., 2015. Data-driven evidential belief modelling of mineral potential using few prospects and evidence with missing values. Nat. Resour. Res. http://dx.doi.org/10.1007/s11053-014-9250-z.

Chandrasekhar, P., Vinod Kumar, V., Martha, T.R., Subramanian, S.K., 2009. Multi earth observation data to identify indicators for mineralized zones in parts of Iran. J. Indian Geophys. Union 13, 133–138.

Eberle, D., Hutchins, D., Das, S., Majumdar, S., Paasche, H., 2015. Automated pattern recognition to support geological mapping and exploration target generation — a case study from southern Namibia. J. Asian Earth Sci. 106, 60–74.

Elipoulolos, M.E., Vacondios, I., 1995. Geochemistry of chromitites and host rocks from the pindos ophiolite complex, northwestern Greece. Chem. Geol. 122, 99–108. http://dx.doi.org/10.1016/0009-2541(94)00154-Z.

Gale, A., Dalton, A.D., Langmuir, C.H., Su, Y., Schilling, J.G., 2013. Themean composition of ocean ridge basalts. Geochem. Geophys. Geosyst. 14, 489–518. http://dx.doi.org/10.1029/2012GC004334.

Ghasemi, H., Juteau, T., Bellon, J., Sabzehei, M., Whitechurch, H., Ricou, L.E., 2002. The mafic–ultramafic complex of Sikhoran (central Iran): a polygenetic ophiolite complex. Compt. Rendus Geosci. 334, 431–438. http://dx.doi.org/10.1016/S1631-0713(02)01770-4.

Ghazi, A.M., Hssanipak, A.A., 1999. Geochemistry and petrography of sub alkaline and alkaline extrusive of Kermanshah ophiolit, Zagros suture zone, SW Iran. J. Asian Earth Sci. 17, 319–332. http://dx.doi.org/10.1016/S0743-9547(98)00070-1.

Ghazi, A.M., Hssanipak, A.A., Wallace, K., 1997. Geochemistry, petrology and geology of the Sabzevar ophiolit, northeastern Iran: implication on tethyan tectonics. Geol. Soc. Am. 29, A-229.

González-Jiménez, J.M., Augé, T., Gervilla, F., Bailly, L., Proenza, J.A., Griffin, W.L., 2011. Mineralogy and geochemistry of platinum rich chromitite from the mantle — crust transition zone at Ouen Island and New Caledonia Ophiolite. Can. Mineral. 49, 1549–1569. http://dx.doi.org/10.3749/canmin.49.6.000.

González-Jiménez, J.M., Griffin, W.L., Proenza, J.A., Gervilla, F., O'Reilly, S.Y., Akbulut, M., Pearson, J.J., Arai, S., 2014. Chromitites in ophiolites: how, where, when, why? Part II. The crystallization of chromitites. Lithos 189, 140–158. http://dx.doi.org/10.1016/j.lithos.2013.09.008.

Happel, U., Hausberg, J., Kisters, A., Meyer, F.M., 1998. The application of digital 3-D ore body modelling to the structural analysis of the Bulqiza–Batra chromite mine, central Albania. Erzmetall 51, 685–692.

Hariri, M.M., 2004. Petrographical and geochemical characteristics of the ultramafic rocks of Jabal Zalm, Central Arabian shield Saudi Arabia. Arab. J. Sci. Eng. 29, 123–133.

Harris, D.P., Pan, G.C., 1990. Subdividing consistent geological areas by relative exceptionalness of additional information, methods and case study. J. Econ. Geol. 85, 1072–1083. http://dx.doi.org/10.2113/gsecongeo.85.5.1072.

Hashim, M., Pournamdary, M., 2011. Processing and interpretation of advanced space-borne thermal emission and reflection radiometer (ASTER) data for lithological mapping in ophiolite complex. Int. J. Phys. Sci. 6, 6410–6421. http://dx.doi.org/10.5897/IJPS11.417.

Hassan, A.A., Kassem, A.M., 2013. Modeling, simulation and performance improvements of a PMSM based on functional model predictive control. Arab. J. Sci. Eng. 38, 3071–3079. http://dx.doi.org/10.1007/s13369-012-0460-6.

Hassanipak, A.A., Ghazi, A.M., 2000. Petrology, geochemistry and tectonic setting of the Khoy ophiolite, Nortwest Iran. J. Asian Earth Sci. 18, 109–121. http://dx.doi.org/10.1016/S1367-9120(99)00023-1.

Hassanipak, A.A., Ghazi, A.M., Wampler, J.M., 1996. REE characteristics and K/Ar ages of the Bande–Ziarat ophiolite complex, southeastern Iran. Can. J. Earth Sci. 33, 1534–1542.

Hofer, C., Kraus, S., Miller, H., Afaro, G., Barra, F., 2001. Chromite-bearing serpentinite bodies within an arc-backark metamorphic complex near La cabana, south Chilean Costal Cordillera. J. S. Am. Earth Sci. 14, 113–126. http://dx.doi.org/10.1016/S0895-9811(01)00011-6.

Jannessary, M.R., Melcher, F., Lodziak, J., Meisel, T.C., 2012. Review of platinum-group element distribution and mineralogy in chromitite ores from southern Iran. Ore Geol. Rev. 48, 278–305. http://dx.doi.org/10.1016/j.oregeorev.2012.05.001.

Kop, A., Ezer, M., Bodur, M.N., Darbaş, M., Inan, S., Ergintav, S., Seyis, C., Yalçin, C., 2014. Geochemical monitoring along the Türkoğlu (Kahramanmaraş)–Gölbaşı (Adıyaman) segments of the east Anatolian fault system. Arab. J. Sci. Eng. 39, 5521–5536. http://dx.doi.org/10.1007/s13369-013-0912-7.

Kuno, A., Matsuo, M., 2000. Characterization of natural chromites samples from ophiolite complexes in the Philippines. Nucl. Chem. 246, 79–83. http://dx.doi.org/10.1023/A:1006724913427.

Li, Nan, Bagas, L., Li, X., Xiao, K., Li, Y., Yinga, L., Song, X., 2016. An improved buffer analysis technique for model-based 3D mineral potential mapping and its application. Ore Geol. Rev. 76, 94–107. http://dx.doi.org/10.1016/j.oregeorev.2015.12.002.

McCuaig, T.C., Hronsky, J.M.A., 2014. The mineral system concept: the key to exploration targeting. Soc. Econ. Geol. Spec. Publ. 18, 153–175.

McCuaig, T.C., Beresford, S., Hronsky, J., 2010. Translating the mineral systems approach into an effective exploration targeting system. Ore Geol. Rev. 38, 128–138.

Mondal, S.K., Ripley, E.M., Chusi, L., Frei, R., 2006. The Genesis of Achaean chromitites from the Nuasahi and Sukinda massifs in the Singhbhum craton. Precambrian Res. 148, 45–66. http://dx.doi.org/10.1016/j.precamres.2006.04.001.

Morishita, T., Maeda, J., Myashita, S., Kumagai, H., Matsumoto, T., Dick, H.J.B., 2007. Petrology of local concentration of chromium spinel in dunite from the slow-spreading Southwest Indian Ridge. Eur. J. Mineral. 19, 871–882. http://dx.doi.org/10.1127/0935-1221/2007/0019-1773.

Moutte, J., 2006. Chromite deposits of the Tiebaghi ultramafic massif, New Caledonia. Econ. Geol. 77, 576–591. http://dx.doi.org/10.2113/gsecongeo.77.3.576.

Najafzadeh, A.R., Ahmadipour, H., 2014. Using platinum-group elements and Au geochemistry to constrain the genesis of podiform chromitites and associated peridotites from the Soghan mafic–ultramafic complex, Kerman, Southeastern Iran. Ore Geol. Rev. 60, 60–75.

Najafzadeh, A.R., Ahmadipour, H., 2016. Geochemistry of Platinum-group elements and mineral composition in chromitites and associated rocks from the Abdasht ultramafic complex, Kerman, Southeastern Iran. Ore Geol. Rev. 75, 220–238. http://dx.doi.org/10.1016/j.oregeorev.2015.12.018.

Najafzadeh, A.R., Arvin, M., Pan, Y., Ahmadipour, H., 2008. Podiform chromitites in the Sorkhband ultramafic complex, Southern Iran: evidence for ophiolitic chromitite. J. Sci. Islam. Repub. Iran 19, 49–65.

Oki, M., Oki, T.K., Charles, E., 2012. Chromate and chromate–phosphate conversion coatings on aluminium. Arab. J. Sci. Eng. 37, 59–64. http://dx.doi.org/10.1007/s13369-011-0157-2.

Pagé, P., Barnes, S.J., 2009. Using trace elements in chromites to constrain the origin of podiform chromitites in the Thetford mines ophiolite, Québec. Econ. Geol. 104, 997–1018. http://dx.doi.org/10.2113/gsecongeo.104.7.997.

Paktunc, A.D., 1990. Origin of podiform chromite deposits by multistage melting, melt segregation and magma mixing in the upper mantle. Ore Geol. Rev. 5, 211–222. http://dx.doi.org/10.1016/0169-1368(90)90011-B.

Pan, G.C., 1989. Concepts and methods of multivariate information synthesis for mineral resource estimation (Ph.D. Dissertation) University of Arizona, Tucson.

Pan, G.C., 2010. Critical issues in mineral resource appraisal. Geol. Bull. China 29 (10), 1413–1429.

Pan, G.C., Harris, D.P., 1992a. Estimating a favorability equation for the integration of geodata and selection of mineral exploration target. J. Math. Geol. 24, 177–202. http://dx.doi.org/10.1007/BF00897031.

Pan, G.C., Harris, D.P., 1992b. Delineation of intrinsic geological unit. J. Math. Geol. 25, 9–39. http://dx.doi.org/10.1007/BF00890673.

Pan, G.C., Harris, D.P., 2000. Information Synthesis for Mineral Exploration. Oxford University Press, pp. 44–70 (Chapter 3).

Parlak, O., Hock, V., Delaloye, M., 2002. The supra-subduction zone Pozanti–Karsanti ophiolite, Southern Turkey: evidence for the high-pressure crystal fractionation of ultramafic cumulates. Lithos 65, 205–224. http://dx.doi.org/10.1016/S0024-4937(02)00166-4.

Peighambari, S., Uysal, I., Stoch, H.G., Ahmadipour, H., Heidarian, H., 2016. Genesis and tectonic setting of ophiolitic chromitites from the Dehsheikh ultramafic complex (Kerman, southeastern Iran): inferences from platinum-group elements and chromite compositions. Ore Geol. Rev. 74, 39–51. http://dx.doi.org/10.1016/j.oregeorev.2015.10.032.

Porwal, A., Carranza, E.J.M., 2015. Introduction to the Special Issue: GIS-based mineral potential modelling and geological data analyses for mineral exploration. Ore Geol. Rev. 71, 477–483. http://dx.doi.org/10.1016/j.oregeorev. 2015.04.017.

Pournamdari, M., Hashim, M., 2013. Detection of chromite bearing mineralized zones in Abdasht ophiolite complex using ASTER and ETM + remote sensing data. Arab. J. Geosci. 7, 1973–1983. http://dx.doi.org/10.1007/s12517-013-0927-0.

Pournamdari, M., Hashim, M., Beiranvand Pour, A., 2014. Application of ASTER and Landsat TM data for geological mapping of Esfandagheh ophiolite complex, southern Iran. Resour. Geol. 64, 233–246. http://dx.doi.org/10.1111/rge.12038.

Proenza, J.A., Gervilla, F., Melgarejo, J.C., Vera, O., Alfonso, P., Fallik, A., 2001. Genesis of sulfide rich chromite ores by the interaction between chromitite and pegmatitic olivine, Norite dikes in the Potosi mine (Moa Baracoa ophiolitic massif, Cuba). Mineral. Deposita 36, 658–669. http://dx.doi.org/10.1007/s001260100193.

Rahgoshay, M., Shafaii Moghadam, H., Forouzesh, V., 2005. Petrology of podiform chromitites in Kuh-Siah, north of Sabzevar. Proceeding of Crystallographic and Mineralogical Conference, Ahwaz, Iran.

Rahgoshay, M., Shafaii Moghadam, H., Monsef, I., Foruzesh, V., 2006. Petrology of podiform chromites in Sabzevar ophiolites, NE of Iran. Geophys. Res. Abstr. 8 (Ref-ID: 1607-7962/gra/EGU06-A-05315).

Rajabzadeh, M.A., Nazari Dehkordi, T., Caran, Ş., 2013. Mineralogy, geochemistry and geotectonic significance of mantle peridotites with high-Cr chromitites in the Neyriz ophiolite from the outer Zagros ophiolite belts, Iran. J. Afr. Earth Sci. 78, 1–15. http://dx.doi.org/10.1007/s00710- 012-0265-z.

Roberts, S., Neary, C., 1993. Petrogenesis of ophiolitic chromitite. Geol. Soc. Lond. Spec. Publ. 76, 257–272.

Rollinson, H., 2008. The geochemistry of mantle chromitites from the northern part of the Oman ophiolite: inferred parental melt composition. Contrib. Mineral. Petrol. 156, 273–288. http://dx.doi.org/10.1007/s00410-008-0284-2.

Saalmann, K., Laine, E.L., 2014. Structure of the Outokumpu ore district and ophiolite-hosted Cu–Co–Zn–Ni–Ag–Au sulfide deposits revealed from 3D modeling and 2D high-resolution seismic reflection data. Ore Geol. Rev. 62, 156–180. http://dx.doi.org/10.1016/j.oregeorev.2014.03.003.

Schiano, P., Masser, D., 1997. Primitive basaltic melts included in podiform chromites from the Oman ophiolite. EPSL 146, 489–497. http://dx.doi.org/10.1016/S0012-821X(96)00254-3.

Shafaii Moghadam, H., Whitechurch, H., Rahgoshay, M., Monsef, I., 2009. Significance of Nain–Baft ophiolitic belt (Iran): short-lived, transtensional Cretaceous backarc oceanic basins over the Tethyan subduction zone. Compt. Rendus Geosci. 341, 1016–1028. http://dx.doi.org/10.1016/j.crte.2009.06.011.

Shafaii Moghadam, H., Rahgooshay, M., Forouzesh, V., 2010a. Geochemical investigation of the noudular chromites in the Forumad ophiolite, NE of Iran. Iran. J. Sci. Technol. Trans. A 33 (A1).

Shafaii Moghadam, H., Stern, R.J., Rahgoshay, M., 2010b. The Dehshir ophiolite (central Iran): geochemical constraints on the origin and evolution of the Inner Zagros ophiolite belt. Geol. Soc. Am. Bull. 122, 1516–1547. http://dx.doi.org/10.1130/B30066.1.

Shafaii Moghadam, H., Mosaddegh, H., Santosh, M., 2013. Geochemistry and petrogenesis of the late Cretaceous Haji-Abad ophiolite (outer Zagros ophiolite belt, Iran): implications for geodynamics of the Bitlis–Zagros suture zone. Geol. J. 48, 579–602. http://dx.doi.org/10.1002/gj.2458.

Shirzadi, A., Masoudi, F., Rahimzadeh, B., 2013. Nature of chromite parent magma in Sabzevar ophiolite (North-East of Iran). Iran. J. Crystallogr. Mineral. 21, 49–58.

Shojaat, B., 1999. Application of geochemical models for determining tectonic environment and potential for ore deposits in Sabzevar ophiolite, North Central Iran (Ph.D. dissertation) Azad University, Tehran, Iran.

Shojaat, B., Hssanipak, A.A., Ghazi, A.M., Mobasher, K., 2003. Petrology, geochemistry and tectonics of the Sabzevar ophiolite, North Central Iran. J. Asian Earth Sci. 19, 1–15. http://dx.doi.org/10.1016/S1367-9120(02)00143-8.

Singh, A.K., 2008. PGE distribution in the ultramafic rocks and chromitites of the Manipur ophiolite complex, Indo–Myanmar orogenic belt, Northeast India. J. Geol. Soc. India 72, 649–660.

Uysal, I., Tarkian, M., Sadiklar, M.B., Zaccarini, F., Meisel, T., Garuti, G., Heidrich, S., 2009. Petrology of Al- and Cr-rich ophiolitic chromitites from the Muğla, SW Turkey: implications from composition of chromite, solid inclusions of platinum-group mineral, silicate, and base-metal mineral, and Os-isotope geochemistry. Contrib. Mineral. Petrol. 158, 659–674. http://dx.doi.org/10.1007/s00410-009-0402-9.

Vatanpour, H.R., Khakzad, A., Ghaderi, M., 2009. Application of PGE in exploration and economic evaluation of Sabzevar ophiolitic belt for chromite deposits. Geosci. Sci. Q. J. 71, 9–12.

Wang, G., Li, R., Carranza, E.J.M., Zhang, S., Yan, C., Zhu, Y., Qu, J., Hong, D., Song, Y., Han, J., Ma, Z., Zhang, H., Yang, F., 2015. 3D geological modeling for prediction of subsurface Mo targets in the Luanchuan district, China. Ore Geol. Rev. 71, 592–610. http://dx.doi.org/10.1016/j.oregeorev.2015.03.002.

Yaghubpur, A., 2005. Mineral deposits of Iran: a brief review. In: Roonwal, G.S., Shahriar, K., Ranjbar, H. (Eds.), Mineral Resources and Development. Daya Publishing House, Delhi-110 035, pp. 191–202.

Yaghubpur, A., Hassannejad, A.A., 2006. The spatial distribution of some chromite deposits in Iran, using fry analysis. J. Sci. 17 (2), 147–152.

Yiğit, O., 2009. Mineral deposits of Turkey in relation to Tethyan metallogeny—implications for future mineral exploration. Econ. Geol. 104, 19–51. http://dx.doi.org/10.2113/gsecongeo.104.1.19.

Zabihi, F., Bozorgmanesh, A.R., 2014. Coefficient estimation for 2D-spline equation, in order to correlate the supercritical rapid expansion process data points. Arab. J. Sci. Eng. 39, 2447–2453. http://dx.doi.org/10.1007/s13369-013-0889-2.